Electrochemistry Communications 115 (2020) 106731

Contents lists available at ScienceDirect

Electrochemistry Communications

journal homepage: www.elsevier.com/locate/elecom

Effect of sp^2 species in a boron-doped diamond electrode on the electrochemical reduction of CO_2

Jing Xu, Yasuaki Einaga*

Department of Chemistry, Keio University, 3-14-1 Hiyoshi, Yokohama 223-8522, Japan

ARTICLE INFO

Keywords:
Boron-doped diamond
sp^2 carbon
CO_2 reduction

ABSTRACT

The effect of sp^2 carbon within a boron-doped diamond (BDD) electrode on the electrochemical reduction of CO_2 is investigated for the first time. With increasing sp^2 content, the Faradaic efficiency for the production of hydrogen (H_2) under constant current density increases while that for the production of formic acid (HCOOH) decreases. Moreover, favorable electrolysis conditions for producing HCOOH shift in the negative potential direction with increasing sp^2 content. This phenomenon is ascribed to the presence of adsorption sites on the sp^2 carbon. This work provides guidance for selectively controlling the reduction of CO_2 by adjusting the distribution of carbonaceous species in the BDD electrode.

1. Introduction

Conversion of CO_2 into value-added chemicals and fuels provides a direct method for making use of the greenhouse gas CO_2. The electrochemical reduction of CO_2 has been comprehensively studied in recent decades and large numbers of mechanisms have been proposed [1,2]. However, during electrochemical reduction, there is an unavoidable competition between CO_2 and proton (H^+) generation in an aqueous electrolyte. Since both the CO_2 reduction reaction (CO_2RR) and the hydrogen evolution reaction (HER) consume electrons [Eqs. (1) and (2)], it is not easy to achieve efficient CO_2RR.

$$CO_2 + e^- \rightarrow CO_2^{\cdot -} \quad E_0 = -1.9\ V \quad (vs.\ NHE) \tag{1}$$

$$2H^+ + 2e^- \rightarrow H_2 \quad E_0 = 0\ V \quad (vs.\ NHE) \tag{2}$$

Boron-doped diamond (BDD) possesses a number of favorable properties for an electrode, including a wide potential window, low background current, chemical inertness and mechanical durability compared to conventional metal electrodes [3]. With its wide potential window, which can suppress HER during electrolysis, BDD is a promising candidate for CO_2RR [4–6]. Effective CO_2RR using a BDD electrode has been demonstrated in previous studies in which formaldehyde was produced using sea-water [6], formic acid was produced using an alkaline solution [4], methanol was produced from an amine solution [7], carbon monoxide was produced using a $KClO_4$ electrolyte [8] and high carbon compounds were produced on metal-modified BDDs [9]. However, these studies focused mainly on the effect of electrolytes or of the working potential; there has been little investigation of the intrinsic characteristics of BDD electrodes.

BDD is composed of carbon atoms with a sp^3-bonded diamond structure, in which some carbon atoms are replaced by boron atoms. Following this replacement, the electrochemical properties change dramatically from insulator to semiconductor [3,10,11]. Generally speaking, the factors that affect the characteristics of the BDD are the boron doping level [12], the presence or absence of sp^2 carbon [13–15] and the surface termination [16]. Amongst these, the presence of sp^2 carbon has a direct effect on the band structure and the density of state (DOS), and would be expected to have a strong influence on the electrochemical properties [17].

BDDs containing sp^2 carbon are normally considered to be of low quality, since they have a greater background current [13] and are easier to corrode [18] than material with no sp^2 carbon. Nevertheless, sp^2-containing BDD has performed very well in a number of applications, including the treatment of waste water [19], oxygen reduction [20], and the generation of ozone [13]. The products of CO_2RR on BDD without sp^2 carbon are mainly HCOOH [4]. However, CO_2RR on sp^2 carbon electrodes such as glassy carbon (GC), graphite, graphene and HOPG has shown a tendency for CO to be the main product [21–24]. This difference in the products of CO_2RR has been reported to be related to the absorbability of the electrode surface [25].

Herein, we have studied CO_2RR on BDD electrodes with various sp^2/sp^3 ratios, which were determined by Raman spectroscopy [14]. BDD containing 0.1% boron was selected as a candidate for further investigation owing to its excellent performance for CO_2RR compared

* Corresponding author.
E-mail address: einaga@chem.keio.ac.jp (Y. Einaga).

https://doi.org/10.1016/j.elecom.2020.106731
Received 2 March 2020; Received in revised form 9 April 2020; Accepted 10 April 2020
Available online 13 April 2020

Table 1
B/C ratio and $I_G/I_{Diamond}$ values of BDDs used in Fig. 4.

B/C ratio (%)	$I_G/I_{Diamond}$		
	no-sp^2	mid-sp^2	high-sp^2
0.03	0	0.02	0.03
0.07	0	0.09	0.11
0.15	0	0.05	0.1
0.70	0	0.04	0.15
2.20	0	0.08	0.09

to BDD electrodes with other B/C ratios [5]. This study should help in elucidating the electrocatalytic properties of the BDD electrode towards the CO_2RR.

2. Experimental

2.1. Preparation of BDD working electrode

BDDs with different carbon sp^2 levels were fabricated by MPCVD (AX6500X, CORNES Technologies corp.). By modifying the gas flow rates of the boron source $B(CH_3)_3$, the carbon source CH_4 and the carrier gas H_2, BDDs with a boron to carbon ratio (B/C) of 0.1% and a variety of sp^2/sp^3 ratios were deposited on silicon wafers as described elsewhere [14]. Commercial GC electrodes (Tokai Corp.) were used for comparison, and were smoothed by grinding before use.

The surface morphology was observed by SEM (JCM-6000, JEOL). Raman spectra were recorded with an excitation wavelength of 532 nm in ambient air at room temperature with an Acton SP2500 (Princeton Instruments). The sp^2/sp^3 ratios ($I_G/I_{Diamond}$) estimated from the Raman data are listed in Table 1. The samples were categorised as no sp^2, mid sp^2 and high sp^2 (details of this assignment are given in [14]). The actual boron content of each BDD was estimated by Glow Discharge Optical Emission Spectroscopy (GDOES) (GD-Profiler2, Horiba Ltd.) with reference to a BDD sample whose boron content had already been estimated by SIMS [13].

2.2. Electrochemical reduction of CO_2

The electrochemical measurements were conducted in a two-compartment flow cell separated with a Nafion membrane (NRE-212, 0.002 in thickness, Aldrich), as described in our previous research [4,5]. The fabricated BDD, Pt plate and Ag/AgCl (in saturated KCl) were used as the working electrode, counter electrode and reference electrode, respectively. The geometric area of both the BDD and Pt electrode were 9.62 cm^2. Prior to every electrochemical measurement, electrochemical pretreatment using cyclic voltammetry (CV) in 0.1 M H_2SO_4 aqueous solution was carried out to ensure that the surface termination was consistent, as described in previous research [4]. Fundamental electrochemical properties such as the potential window and the CV performed in redox electrolytes were as shown in other reports [14].

The electrochemical reduction of CO_2 was performed as follows. The catholyte and anolyte were aqueous solutions of 0.5 M KCl and 1 M KOH, respectively. Both were 50 mL solutions and were circulated separately in the cell with a flow rate of 100 mL min^{-1} using separate pumps. The catholyte was purged with N_2 gas for 30 min at 200 sccm to remove any dissolved oxygen and then bubbled with CO_2 gas for 1 h at 500 sccm to saturate it with CO_2. After N_2 and CO_2 saturation, linear sweep voltammetry (LSV) measurements were carried out in the potential range from −1 V to −3.5 V (vs. Ag/AgCl) at 0.02 V s^{-1}. The chronopotentiometry reductions were performed under a constant current density of −2 mA cm^{-2} for 1 h. The chronoamperometry reductions were at −2.2 V, −2.5 V, −2.7 V, −2.9 V and −3.4 V (vs. Ag/AgCl) for 1 h. During the reduction, CO_2 was continually bubbled into the catholyte at a slow flow rate. After the electrolysis, N_2 gas was bubbled into the catholyte for 15 min at 50 sccm and the gaseous products collected in an aluminum bag (CEK 3008–26401, GL Science). The H_2 and CO produced were analyzed by gas chromatography (GC-2014, Shimadzu Corp.) while the HCOOH was analyzed by high-performance liquid chromatography (HPLC, Prominence, Shimadzu Corp.). The Faradaic efficiency was estimated from the yield of each product, as described elsewhere [4].

3. Results and discussion

3.1. Characterization of the BDDs

Basic characterization results for the samples, such as the actual B/C ratio, $I_G/I_{Diamond}$ and the average grain size have been reported in a previous study [14]. It is important to emphasise that the actual B/C ratios of the three BDDs studied (0.08%, 0.06% and 0.07%) are roughly equal to each other, and therefore any drastic change in electrochemical reduction could not be due to a difference in the boron content of the electrodes. The $I_G/I_{Diamond}$ ratios (0, 0.09 and 0.11) were obtained by Raman analysis. Each sample revealed a clear first-order diamond peak at 1332 cm^{-1}. A broad band around 1550 cm^{-1} was found in the spectra of mid-sp^2 and high-sp^2 BDD, which confirms the presence of sp^2 sites (amorphous carbon and graphitic carbon). By contrast, the no-sp^2 BDD showed a negligible level of sp^2 defects. Furthermore, using SEM, the average grain size of the BDDs (13.0, 10.6 and 9.5 μm) was found to decrease with increasing sp^2 content. Additionally, there are more boundaries on sp^2-containing BDD [26,27] than in the sp^2-free diamonds. This indicates that secondary nucleation is extended by enhancing the sp^2 character [17].

3.2. CO_2RR on sp^2-containing BDDs

3.2.1. LSV before and after CO_2 bubbling

The electrocatalytic activity of the BDDs was examined in CO_2-saturated 0.5 M KCl solutions. The LSV curves before and after CO_2 bubbling are shown in Fig. 1, in which the potential was swept between −1 V and −3.5 V (vs. Ag/AgCl) at a rate of at 0.02 V s^{-1}.

Comparing the LSVs with increasing sp^2 content after CO_2 bubbling in Fig. 1 (solid lines), two clear changes in the voltammograms are noticeable. There is an obvious negative shift of the onset potential from −2.3 V to −2.6 V and −3.4 V (vs. Ag/AgCl) with increasing sp^2 content. On the other hand, a sizeable decrease in the anodic current at −3.5 V was observed from approximately 45 mA cm^{-2} to 7 mA cm^{-2} and 1 mA cm^{-2} in samples with increasing sp^2 content. The measured current

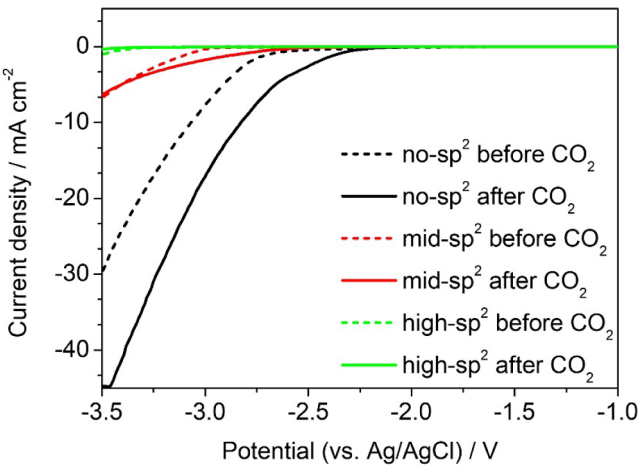

Fig. 1. Electrochemical performance of different electrodes by mean of an LSV scan with a scan rate of 0.02 V s^{-1} in 0.5 M KCl aqueous electrolyte before and after CO_2 saturation.

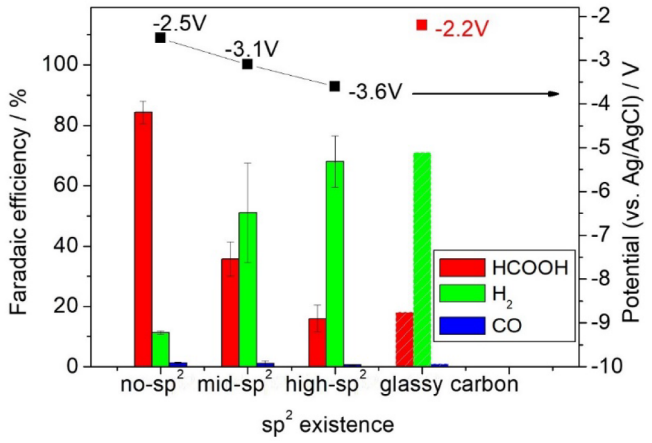

Fig. 2. Faradaic efficiency of CO_2RR on different electrodes and the corresponding potential, under a constant current density of -2 mA cm^{-2} for a 1 h reduction.

was composed of two parts: partial current from HER and partial current from CO_2RR. One possible reason for the negative shift in the potential and decreased current is the diminished carrier density caused by the increasing sp^2/sp^3 ratio [14], which also inhibits the CO_2RR activity.

3.2.2. Reduction with constant current density

Fig. 2 shows the products of CO_2RR and the corresponding reduction potentials on various BDD electrodes and also on a GC electrode. The results were obtained at constant current density of -2 mA cm^{-2} for 1 h. It can be seen that the tendency towards HCOOH production decreases with increasing sp^2 content, while the tendency towards H_2 production increased. The results show the reduction potential shifting to more negative values with increasing sp^2 content. The reduction potential decreased from –2.5 V to -3.1 V and -3.6 V (vs. Ag/AgCl) for no-sp^2, mid-sp^2 and high-sp^2 electrodes, respectively, which to some extent agrees with the LSV results in Fig. 1.

As indicated by previous studies, HCOOH is the main product of CO_2RR by BDD electrodes with little sp^2 content [4,5]. This is also shown by the data for no-sp^2 BDD in Fig. 2, for which the Faradaic efficiency was as high as 84% for HCOOH. The performance of mid-sp^2 BDDs, at 36% efficiency for producing HCOOH, was not as high as for the no-sp^2 BDD electrode. Rather like GC electrodes, which contain sp^2 over the entire surface and have 18% efficiency for HCOOH, high-sp^2 BDD had a 16% HCOOH efficiency. However, H_2 evolution increased with increasing sp^2 content, with efficiency values of 11% for no-sp^2 BDD, 51% for mid-sp^2 BDD, 68% for high-sp^2 BDD and 71% for GC, respectively. These results suggest that the amount of sp^2 carbon present has a significant influence on the selectivity of the CO_2RR [28].

3.2.3. Potential dependence

Fig. 3 shows the dependence of the Faradaic efficiency on the electrode potential from -4 V to -2.2 V (vs. Ag/AgCl) for each electrode. With increasing sp^2 content, the optimized potential for maximum production of HCOOH moves to a more negative potential. Furthermore, the maximum Faradaic efficiency value for producing HCOOH decreases. As can be seen in Fig. 3(a), the highest Faradaic efficiencies for HCOOH for no-sp^2, mid-sp^2 and high-sp^2 electrodes were obtained at constant potentials of -2.5 V, -2.9 V and -3.4 V (vs. Ag/AgCl), respectively. These values are in accordance with the onset potentials measured by the LSV curves in Fig. 1. The Faradaic efficiencies were correspondingly reduced to 78%, 62% and 12%, respectively.

The minimum Faradaic efficiency for H_2 also revealed a negative potential shift. The no-sp^2 BDD sample produced the least H_2 at -2.5 V (vs. Ag/AgCl), while the corresponding high sp^2 and mid sp^2 values were -2.7 V and -2.9 V (vs. Ag/AgCl), respectively.

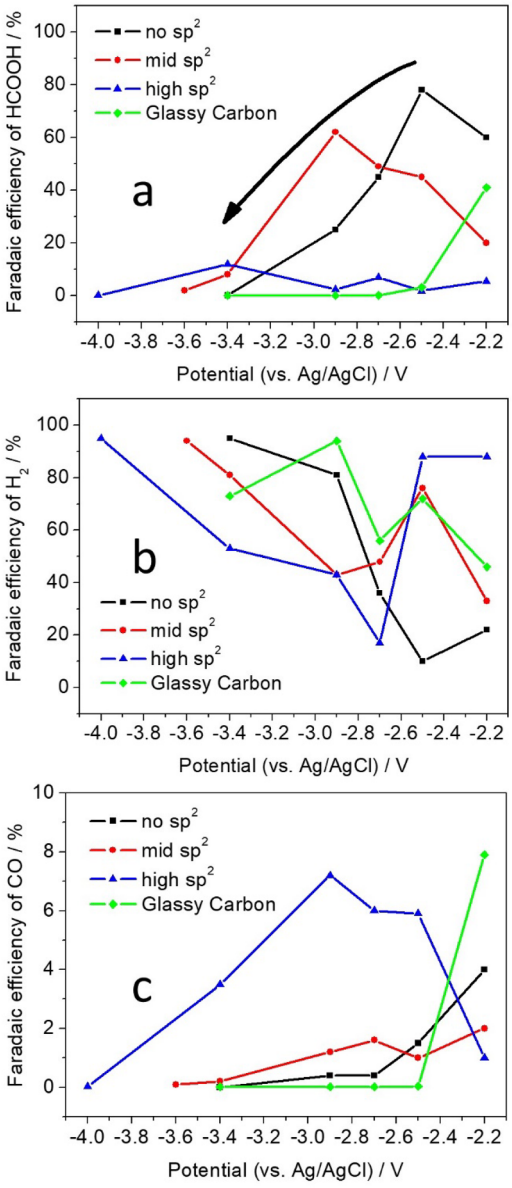

Fig. 3. Faradaic efficiency of generating (a) HCOOH, (b) H_2 and (c) CO on different electrodes under a constant potential from -4 V to -2.2 V (vs. Ag/AgCl) respectively.

The Faradaic efficiency for production of CO on all electrodes was lower than 10%. However, the high-sp^2 BDD produced more CO than the other BDDs in the potential range from -3.4 V to -2.5 V (vs. Ag/AgCl). The highest Faradaic efficiency of high-sp^2 BDD is 7% at a potential of -2.9 V (vs. Ag/AgCl). The results indicate that a CO_2RR producing CO is easier to obtain on BDDs containing sp^2 species than on BDDs with no sp^2 carbon.

3.3. Mechanism proposal

The presence of sp^2 carbon clearly affects the rate of reduction of CO_2 under constant current, which is a competition between CO_2RR and HER. For BDD electrodes in the absence of sp^2 carbon, HCOOH is the major product, whilst H_2 is a minor product. Our results indicate that CO_2RR performs much better than HER on a sp^3 surface. This phenomenon is ascribed to the wide potential window of BDD, allowing the HER to be minimized and CO_2RR to become the main reaction [4]. The yield of H_2 is changed a great deal on varying the applied potential,

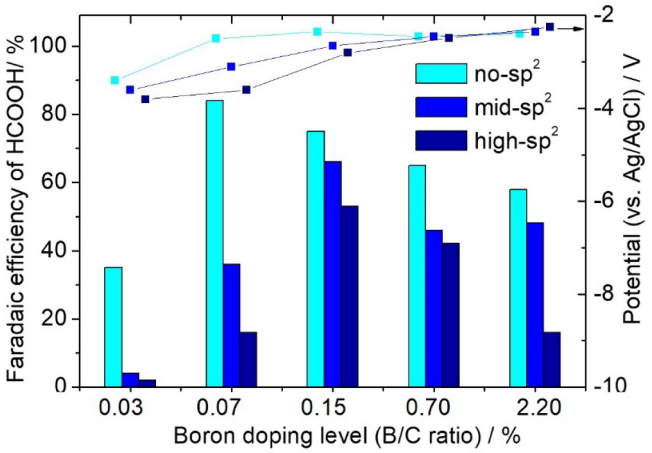

Fig. 4. Faradaic efficiency of HCOOH on electrodes with different boron doping/sp^2 content and the corresponding potentials under a constant current density of -2 mA cm^{-2} for a 1 h reduction.

which indicates that the HER on this electrode is sensitive to potential. By contrast, the BDD electrodes containing sp^2 species produced more H_2 than HCOOH. This distribution of products is probably affected by the adsorption sites present on sp^2 carbon [29].

The product of CO_2RR is a mixture of HCOOH and CO. On BDD electrodes without sp^2 species, HCOOH is the main outcome and CO is a minor product. On the other hand, BDD electrodes containing sp^2 produce a smaller amount of HCOOH and a relatively higher amount of CO. It is suggested that the sp^2 surface has a higher adsorption of $CO_2^{\cdot -}$ and that affects the products of the CO_2RR [25]. It has previously been suggested that CO is generated on adsorbing electrode surfaces whilst HCOOH is produced on surfaces that do not show adsorption [8,30].

The sp^2 effect on the CO_2RR is found not only on the 0.1% BDDs, but also on other samples with different boron content. Fig. 4 shows the Faradaic efficiency for the production of HCOOH on BDD electrodes with various sp^2 content and with different B/C ratios (as listed in Table 1). For each boron doping level, HCOOH production efficiency declined with increasing sp^2 content.

4. Conclusion

We have studied the influence of sp^2 carbon in BDD electrodes on the CO_2RR. BDDs with different sp^2/sp^3 ratios were produced by MPCVD and used as electrodes for CO_2RR. The products were found to demonstrate certain trends with increasing sp^2 content. We observe that, there is a sharp decline in the production of HCOOH with increasing sp^2 content. On the other hand, the yield of H_2 was significantly raised. The results for BDD electrodes with high sp^2 content were similar to those of a well-known sp^2 electrode (GC). Moreover, our results revealed a negative shift in the onset potential for the reduction and a lower maximum yield of HCOOH with increasing sp^2 content. It is suggested that the surface of sp^2-containing BDDs could absorb $CO_2^{\cdot -}$ more easily than those without sp^2 species, although further investigation is required. It is noteworthy that the selectivity of CO_2RR could be controlled by adjusting the distribution of carbonaceous species within the BDD electrode.

CRediT authorship contribution statement

Jing Xu: Conceptualization, Methodology, Investigation, Writing - original draft, Visualization. **Yasuaki Einaga:** Conceptualization, Validation, Writing - review & editing, Supervision.

Acknowledgement

This work is supported by JST (Japan Science and Technology Agency – ACCEL (Strategic Basic Research Programs): Fundamentals and Applications of Diamond Electrodes.

References

[1] N. Yang, S. Yu, J.V. Macpherson, Y. Einaga, H. Zhao, G. Zhao, G.M. Swain, X. Jiang, Chem. Soc. Rev. 48 (2019) 157–204.
[2] D.D. Zhu, J.L. Liu, S.Z. Qiao, Adv. Mater. 28 (2016) 3423–3452.
[3] Y. Einaga, J. Appl. Electrochem. 40 (2010) 1807–1816.
[4] K. Natsui, H. Iwakawa, N. Ikemiya, K. Nakata, Y. Einaga, Angew. Chem. Int. Ed. 57 (2018) 2639–2643.
[5] J. Xu, K. Natsui, S. Naoi, K. Nakata, Y. Einaga, Diam. Relat. Mater. 86 (2018) 167–172.
[6] K. Nakata, T. Ozaki, C. Terashima, A. Fujishima, Y. Einaga, Angew. Chem. Int. Ed. 53 (2014) 871–874.
[7] P.K. Jiwanti, K. Natsui, K. Nakata, Y. Einaga, RSC Adv. 6 (2016) 102214–102217.
[8] M. Tomisaki, S. Kasahara, K. Natsui, N. Ikemiya, Y. Einaga, J. Am. Chem. Soc. 141 (2019) 7414–7420.
[9] P.K. Jiwanti, K. Natsui, K. Nakata, Y. Einaga, Electrochim. Acta 266 (2018) 414–419.
[10] A. Fujishima, Y. Einaga, T.N. Rao, D.A. Tryk (Eds.), Diamond Electrochemistry, Elsevier B.V, Tokyo, 2005.
[11] J.P. Lagrange, A. Deneuville, E. Gheeraert, Diam. Relat. Mater. 7 (1998) 1390–1393.
[12] K. Schwarzová-Pecková, J. Vosáhlová, J. Barek, I. Šloufová, E. Pavlova, V. Petrák, J. Zavázalová, Electrochim. Acta 243 (2017) 170–182.
[13] T. Watanabe, Y. Honda, K. Kanda, Y. Einaga, Phys. Status Solidi 211 (2014) 2709–2717.
[14] J. Xu, Y. Yokota, R.A. Wong, Y. Kim, Y. Einaga, J. Am. Chem. Soc. 142 (2020) 2310–2316.
[15] J. Li, C.L. Bentley, S.Y. Tan, V.S.S. Mosali, M.A. Rahman, S.J. Cobb, S.X. Guo, J.V. Macpherson, P.R. Unwin, A.M. Bond, J. Zhang, J. Phys. Chem. C 123 (2019) 17397–17406.
[16] S. Kasahara, K. Natsui, T. Watanabe, Y. Yokota, Y. Kim, S. Iizuka, Y. Tateyama, Y. Einaga, Anal. Chem. 89 (2017) 11341–11347.
[17] J.A. Bennett, J. Wang, Y. Show, G.M. Swain, J. Electrochem. Soc. 151 (2004) E306–E313.
[18] T. Kashiwada, T. Watanabe, Y. Ootani, Y. Tateyama, Y. Einaga, ACS Appl. Mater. Interfaces 8 (2016) 28299–28305.
[19] C.D.N. Brito, D.M. de Araújo, C.A. Martínez-Huitle, M.A. Rodrigo, Electrochem. Commun. 55 (2015) 34–38.
[20] T.L. Read, S.J. Cobb, J.V. Macpherson, ACS Sensors 4 (2019) 756–763.
[21] K. Hara, A. Kudo, T. Sakata, J. Electroanal. Chem. 421 (1997) 1–4.
[22] N. Sreekanth, M.A. Nazrulla, T.V. Vineesh, K. Sailaja, K.L. Phani, Chem. Commun. 51 (2015) 16061–16064.
[23] N. Yang, S.R. Waldvogel, X. Jiang, A.C.S. Appl, Mater. Interfaces 8 (2016) 28357–28371.
[24] P. Han, X. Yu, D. Yuan, M. Kuang, Y. Wang, A.M. Al-Enizi, G. Zheng, J. Colloid Interface Sci. 534 (2019) 332–337.
[25] A. Goeppert, M. Czaun, J.-P. Jones, G.K. Surya Prakash, G.A. Olah, Chem. Soc. Rev. 43 (2014) 7995–8048.
[26] J.V. Macpherson, Phys. Chem. Chem. Phys. 17 (2015) 2935–2949.
[27] T. Watanabe, S. Yoshioka, T. Yamamoto, H. Sepehri-Amin, T. Ohkubo, S. Matsumura, Y. Einaga, Carbon 137 (2018) 333–342.
[28] D. Medeiros de Araújo, P. Cañizares, C.A. Martínez-Huitle, M.A. Rodrigo, Electrochem. Commun. 47 (2014) 37–40.
[29] S. Garcia-Segura, E. Vieira dos Santos, C.A. Martínez-Huitle, Electrochem. Commun. 59 (2015) 52–55.
[30] Y. Hori, H. Wakebe, T. Tsukamoto, O. Koga, Electrochim. Acta 39 (1994) 1833–1839.